129.25, 125.08 (aryl C), 79.94 (CNO_2), 74.53 (CHPh), 28.95 (spiro C), 9.45 (CH_2), 8.27 (CH_2). Anal. Calcd for $C_{19}H_{18}N_2O_6$: C, 61.62; H, 4.90; N, 7.57. Found: C, 61.22; H, 4.76; N, 7.62.

Dinitrospiropentane **8** was obtained in 49% yield when **5** (11 mg, 0.07 mmol) was added to an LDA (0.5 mmol) solution at −78 °C with stirring for 1 h, followed by addition of PhCHO (0.08 mL, 0.75 mmol) and continuation of the reaction as above.

pK_a of Dinitrospiropentane 5. Spectrophotometric Experiments.[14a] All solutions were weighed directly in the reaction vessels to determine the quantity of added material. Dimsyl potassium solutions (0.1 M) were freshly prepared from KH (35% mineral oil suspension, washed with three portions of hexanes) and distilled, degassed (Ar stream) DMSO. A DMSO solution of fluorene (45.9 mg in 7.88 g of solution) was added in small aliquots (at least six) to the dimsyl potassium solution, with the absorptions at 517 and 455 nm being used to construct a Beer's law plot: the plot was used to determine the concentration of fluorene anion. Excess fluorene was added in all cases prior to the addition of small aliquots of a DMSO solution of **5** (9.5 mg in 11.01 g of solution). The nitronate concentration was determined by the disappearance of fluorene anion, measured spectroscopically.

Isolation Experiments. Dimsyl potassium solution (0.75 mL, 0.11 M, 0.08 mmol of dimsyl potassium) was added to a stirred solution of the conjugate acid (Table I, 0.6 mmol) in DMSO (4 mL). After 4 min, a solution of **5** (2 mg, 0.01 mmol) in DMSO (2 mL) was added. After 10–16 min of additional stirring, the reaction solution was worked up by the general procedure. Results are shown in Table I.

X-ray Structure Determination of Dinitrospiropentane 5. X-ray intensity data were collected on an Enraf-Nonius CAD4 diffractometer employing graphite-monochromated Cu K_α radiation (λ = 1.541 84 Å) and using the ω–2θ scan technique. A total of 673 reflections were measured over the following ranges: $4 \le 2\theta \le 130°$, $0 \le h \le 13$, $0 \le k \le 7$, $-11 \le l \le 11$. Three standard reflections measured every 3500 s of X-ray exposure showed no intensity decay over the course of data collection. The intensity data were corrected for Lorentz and polarization effects but not for absorption. Of the reflections measured, a total of 551 unique reflections with $F^2 > 3\sigma(F^2)$ were used during subsequent structure refinement. The structure was solved by direct methods (MULTAN11/82). Refinement was by full-matrix least-squares techniques based on F to minimize the quantity $\sum w(|F_o| - |F_c|)^2$ with $w = 1/\sigma^2(F)$. Non-hydrogen atoms were refined anisotropically, and hydrogen atoms were included as constant contributions to the structure factors and were not refined. Refinement converged to R_1 = 0.052 and R_2 = 0.094.

Acknowledgment. The authors thank Dr. William P. Dailey (University of Pennsylvania) for valuable discussions.

Registry No. 1a, 136476-39-6; **1b**, 136476-38-5; **2**, 136476-32-9; **3**, 136476-33-0; **4a**, 136476-40-9; **5**, 136476-35-2; **6a**, 136476-42-1; **6b**, 136476-43-2; **7**, 136476-36-3; **8**, 136476-37-4; 1,1-cyclopropanedicarboxylic acid, 598-10-7; 1-(nitrometyyl)-1-cyclopropanecarboxaldehyde, 136476-34-1; 2benzaldehyde, 100-52-7; 1,1-bis(hydroxymethyl)cyclopropane, 39590-81-3; 1,1-cyclopropanedicarboxaldehyde, 136476-41-0.

Supplementary Material Available: Tables of crystallographic refined positional parameters, refined displacement (β) parameters, and bond distances and angles (4 pages). Ordering information is given on any current masthead page.

Electrochemical Generation and Reduction of Organic Free Radicals. α-Hydroxybenzyl Radicals from the Reduction of Benzaldehyde

Claude P. Andrieux, Maria Grzeszczuk,[1] and Jean-Michel Savéant*

Contribution from the Laboratoire d'Electrochimie Moléculaire de l'Université de Paris 7, Unité Associée au CNRS No. 438, 2 place Jussieu, 75251 Paris Cedex 05, France.
Received May 28, 1991

Abstract: Careful analysis of the kinetics of the electrochemical reduction of benzaldehyde in ethanolic buffers, paying particular attention to the second reduction step(s), shows that the α-hydroxybenzyl radicals formed upon protonation of the initial ketyl radicals are more difficult to reduce than the starting molecule. Thus, a clear example is provided of the lack of general validity of the commonly accepted view that radicals resulting from the addition of electrophiles onto anion radicals should be easier to reduce than the substrate from which they derive. There is then no general impediment to the generation and redox characterization of radicals by electrochemical means along this type of reaction sequence. The main thermodynamic and kinetic characteristics of the reduction, dimerization, and proton exchange interconversion of the α-hydroxybenzyl and benzaldehyde ketyl radicals are derived from the experimental data.

Neutral free radicals may be generated upon electrochemical reduction of organic substrates either directly by dissociative electron transfer or from chemical transformation of an initially formed anion radical. Once formed, these free radicals may in both cases undergo an electron transfer from the electrode surface, leading to the corresponding carbanions. In the second case, they may also be reduced in the solution by electron transfer from the parent anion radicals. The relative value of the reduction potentials of the substrate and of the resulting neutral radical is an essential factor governing the possibility of triggering either a radical or a carbanion chemistry by electrochemical reduction of organic substrates. More generally, gathering thermodynamic and kinetic data on the redox properties of organic free radicals is certainly an important task in radical chemistry from both a mechanistic and a synthetic point of view. For this purpose, an elegant method has been recently developed in which the radical is generated photochemically and characterized electrochemically.[2] If possible, i.e., in the case where the reduction potential of the radical would be more negative than that of the substrate, the use of standard electrochemical techniques such as cyclic voltammetry for both generating the radical and measuring its electrochemical properties would also be a quite valuable tool.[3]

(1) Permanent address: Institute of Chemistry, University of Wroclaw, Poland.

(2) (a) The sensitivity of the technique is greatly enhanced by the use of modulated light combined with in-phase electrochemical detection.[2b] (b) Wayner, D. D. M.; Griller, D. *J. Am. Chem. Soc.* **1985**, *107*, 7764. (c) Wayner, D. D. M.; McPhee, D. J.; Griller, D. *J. Am. Chem. Soc.* **1988**, *110*, 132. (d) Sim, B. A.; Griller, D.; Wayner, D. D. M. *J. Am. Chem. Soc.* **1989**, *111*, 754. (e) Griller, D.; Martinho Simoes, J. A.; Mulder, P.; Sim, B. A.; Wayner, D. D. M. *J. Am. Chem. Soc.* **1989**, *111*, 7872.

0002-7863/91/1513-8811$02.50/0

So far there have been very few systematic estimations of the relative values of the reduction potentials of free radicals and of the substrates from which they may be generated electrochemically. They have mainly concerned radicals that are formed by reductive cleavage reactions, with halide ion as the nucleofugic group in most cases.[4] There is then a sharp difference between the behavior of aromatic and aliphatic halides. In the former case, electron transfer and breaking of the carbon–halogen bond are stepwise, and the aryl radicals thus formed are much easier to reduce than the starting aryl halides. The high reducibility of the aryl radicals does not, however, preclude the possibility of triggering a radical chemistry by electrochemical reduction of aryl halides.[5] The anion radical of the aromatic halide is indeed an intermediate in the reaction, and thus the aryl radical is formed in the solution rather than at the electrode surface, giving it time to react with reagents dispersed in the solution before diffusing back to the electrode surface and being reduced there. Reduction of the aryl radical, however, remains a highly competitive pathway, the more so the faster the cleavage of the carbon–halogen bond. Reduction of the aryl radical also occurs in the solution, if only by electron transfer from the anion radical of the aromatic halide.

In the case of simple aliphatic halides[4] or perfluoroalkyl halides,[5b] the radical is generated along a concerted electron-transfer–bond-breaking reaction. The relative location of the reduction potentials of the substrate and of the radical depends upon the nature of the halogen and of the radical. *tert*- and *sec*-Butyl radicals as well as linear perfluoroalkyl radicals are more difficult to reduce than the parent iodides. *n*-Bu$^{\bullet}$ is easier to reduce than *n*-BuI and *n*-BuBr, and *sec*-Bu$^{\bullet}$ is easier than *sec*-BuBr, whereas *tert*-Bu$^{\bullet}$ and *tert*-BuBr as well as $CF_3^{\bullet}$ and CF_3Br have approximately the same reduction potentials.

The alkyl and perfluoroalkyl iodides thus provide counterexamples of a tacitly accepted rule that states that neutral radicals generated from an organic substrate by means of an electron transfer accompanied by the expulsion of a nucleophile or the addition of an electrophile (including the proton) are easier to reduce than the substrate. An intuitive justification of this rule, which is indeed followed in a number of cases, is that after addition of the first electron the expulsion of the nucleophile or the addition of the electrophile grossly amounts to the loss of an electron pair, thus leading to a species that readily accepts an additional electron. In fact. the only theoretical justification of this rule concerns the reduction of alternate aromatic hydrocarbons and of the radicals they generate by addition of one electron and one proton.[6] Moreover, if justified, the above rule should in fact stand for thermodynamic standard potentials. The actual reduction potentials of both the radical and parent substrates are in addition governed by the kinetics of the electron-transfer steps and by those of the various accompanying chemical reactions.

The aim of the study reported here was to search for examples of the nonapplicability of the above rule in the case where the neutral radical is generated from the substrate by the transfer of one electron and one proton rather than by reductive cleavage. For this purpose we selected the reduction of benzaldehyde in ethanol, for which previous studies have shown that the number of electrons exchanged by molecule is one, shifting from acidic to basic pH, as expected for an electrodimerization reaction leading to the pinacol.[7]

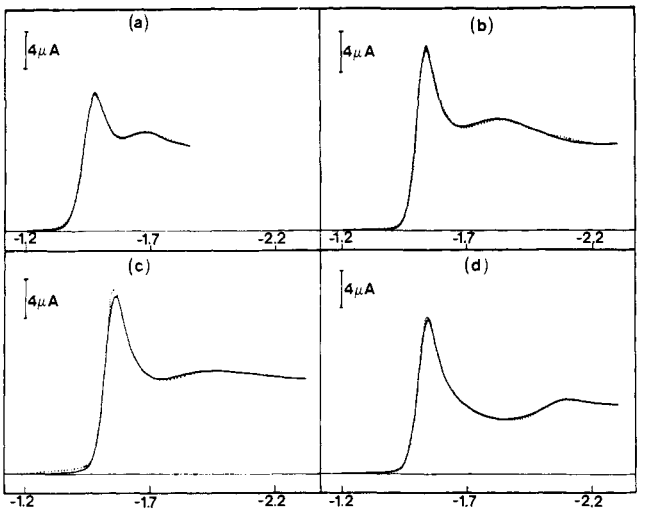

Figure 1. Cyclic voltammograms of benzaldehyde (2 mM) in ethanol at a hanging mercury drop electrode. Scan rate: 1 V s^{-1}. Temperature: 25 °C. pH: 8.2 (a), 10.2 (b), 11 (c), 12 (d). Full lines, experimental curves; dotted lines, simulated curves.

Results and Discussion

In previous studies of the electrochemical reduction of benzaldehyde, emphasis was laid on the variation of the first reduction wave with various parameters such as scan rate, concentration, and pH.[7] In the present study, we gave particular attention to the second wave, at which the reduction of the anion radical or possibly of the neutral radical resulting from its protonation occurs, although the variations of the first wave were also utilized in the analysis of the kinetic data. We used four different buffers obtained from the half-neutralization of veronal (pH 8.2[8]), phenol (pH 10.2[8]), and 2,6-dimethylphenol (pH 11[8]) by a 0.1 M ethanolic solution of *n*-Bu_4NOH and from a solution of 0.05 M *n*-Bu_4NOH and 0.05 M *n*-Bu_4NClO_4 (pH 12[8]). The cyclic voltammetry of a solution of benzaldehyde in each of these four buffers was investigated at a hanging mercury drop electrode at scan rates ranging between 0.1 and 1000 V s^{-1} with positive feedback compensation of the ohmic drop. Figure 1 shows the results obtained at 1 V s^{-1}. These data provide the first qualitative clue that the α-hydroxybenzyl radical resulting from the protonation of the initially formed ketyl radical is not easier to reduce than the starting benzaldehyde. In all buffers, the second waves are small, as expected for the reduction of transient intermediates.[3] There is little doubt that, in the most basic buffer, the second wave represents the reduction of the ketyl radical, $PhCHO^{\bullet-}$, generated at the first wave; the first wave becomes reversible at about 100 V s^{-1} and, simultaneously, the second increases in height so as to reach the height corresponding to the one-electron reduction of a stable species. As seen in Figure 1, the second wave undergoes a considerable positive shift upon decreasing the pH: its peak potential goes from −2.09 to −1.67 V vs SCE from pH 12 to pH 8.2. Such a large shift is not compatible with the assignment of the second wave to the reduction of the benzaldehyde ketyl (reaction e2), even taking into account that the electron-transfer step is followed by protonation steps. Although not very probable, the most favorable conditions for a maximal variation of the peak

(3) (a) Andrieux, C. P.; Savéant, J.-M. *J. Electroanal. Chem.* **1989**, *267*, 15. (b) Andrieux, C. P.; Gallardo, I.; Savéant, J.-M. *J. Am. Chem. Soc.* **1989**, *111*, 1620.

(4) (a) See ref 4b and references cited therein. For reviews on the electrochemistry of organic halides, see refs 4c and 4d. (b) Savéant, J.-M. *Adv. Phys. Org. Chem.* **1990**, *26*, 1. (c) Hawley, M. D. In *Encyclopedia of Electrochemistry of the Elements*; Bard, A. J., Lund, H., Eds.; Marcel Dekker: New York, 1980; Vol. XIV, Organic Section. (d) Becker, J. Y. *The Chemistry of Functional Groups, Suppl. D*; Patai, S., Rappoport, Z., Eds.; Wiley: New York, 1983; Chapter 6, pp 203–285.

(5) (a) For example, H-atom transfer from the solvent or reaction with nucleophiles leading to an electrochemically induced aromatic nucleophilic substitution.[4a] (b) Andrieux, C. P.; Gélis, L.; Médebielle, M.; Pinson, J.; Savéant, J.-M. *J. Am. Chem. Soc.* **1990**, *112*, 3509.

(6) (a) From Hückel quantum chemical calculations.[6b] (b) Hoijtink, G. J.; Van Schooten, J.; de Boer, E.; Aalberberg, W. Y. *Recl. Trav. Chem. Pays-Bas* **1954**, *73*, 355. (c) In this particular case, the theoretical prediction seems to be indeed followed experimentally.[6d] (d) Peover, M. E. In *Electroanalytical Chemistry*; Bard, A. J., Ed.; Marcel Dekker: New York, 1967; Vol. 2, pp 1–51.

(7) (a) Mairanovskii, S. G. *Izv. Akad. Nauk SSSR* **1961**, 2140. (b) Savéant, J.-M.; Vianello, E. *C. R. Acad. Sci.* **1963**, *256*, 2597. (c) Laviron, E. *Coll. Czech. Chem. Commun.* **1965**, *30*, 4219. (d) Nadjo, L.; Savéant, J.-M. *J. Electroanal. Chem.* **1971**, *33*, 429. (e) Hayes, J. W.; Ruzic, I.; Smith, D. E.; Booman, G. L.; Delmastro, J. R. *J. Electroanal. Chem.* **1974**, *51*, 269. (f) Savéant, J.-M.; Tessier, D. *J. Phys. Chem.* **1978**, *82*, 1723. (g) Evans, D. H. In *Encyclopedia of Electrochemistry of the Elements*; Bard, A. J., Lund, H., Eds.; Marcel Dekker: New York, 1978; Vol. XII, Organic Section, pp 3–259. (h) Parker, V. D.; Lerflaten, O. *Acta Chem. Scand. B* **1983**, *37*, 403.

(8) As measured with an aqueous glass electrode.

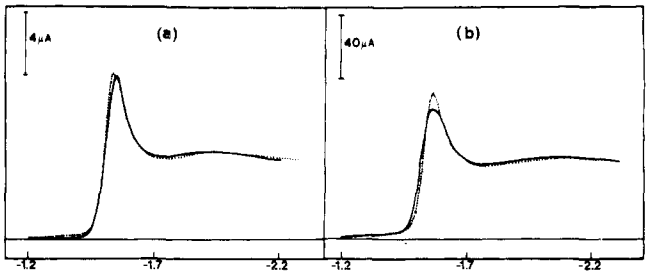

Figure 2. Cyclic voltammograms of benzaldehyde (2 mM) in ethanol at a hanging mercury drop electrode. Temperature: 25 °C. pH: 11. Scan rate: 0.5 V s^{-1} (a), 50 V s^{-1} (b). Full lines, experimental curves; dotted lines, simulated curves.

potential of the second wave would involve a fast electron transfer (e3) and a followup proton transfer such that the reverse reaction would be at the diffusion limit. The shift would be (30 mV per decade of the pseudo-first-order rate constant[9]) 112 mV, i.e., much smaller than the value (420 mV) observed experimentally. In addition to that, the electron-transfer step in reaction e3 is so slow as to be totally irreversible, as will be made clear in the following. Under these conditions, the decrease in pH would not result in any shift of the wave since a step preceding the protonation reactions would be rate-determining.

We also note that, at pH 11, the second wave is drawn out in such a way that it appears as the sum of two successive waves. We are thus led to conclude that, while the second wave observed at pH 12 represents the reduction of the ketyl radical, those that are seen at pH 10.2 and 8.2 correspond to the reduction of the α-hydroxybenzyl radical. The two waves observed at pH 11 thus correspond to a "CE" type reduction[9] of the α-hydroxybenzyl and ketyl radicals. The former is reduced first and a part of the second is reduced at the same potential by displacement reaction p, whereas the most negative wave corresponds to the reduction of the remainder of the ketyl radicals. The two waves are of comparable height at 1 V s^{-1}, resulting in a broad merged wave (Figure 1). They are more visible individually at a low scan rate for the hydroxy radical wave and at a high scan rate for the ketyl radical one (Figure 2). In the simulation of Figure 2b, the peak height for the reduction wave of benzaldehyde is significantly lower than the experimental height. This is due to the onset of the reversibility of that wave, which fully appears at pH 12.[10]

It thus appears that the reduction of benzaldehyde does provide an example where the neutral radical formed upon a $1e^- + 1H^+$ transfer *is not* easier to reduce than the starting molecule.

We now analyze the reaction mechanism in a more quantitative manner. The data concerning the first wave are useful in this connection. As seen in Figure 3, the peak potential of the first wave varies by about 20 mV per decade of scan rate at pH 12, 11, and 10.2, indicating that the first electron-transfer step is followed by a reaction that formally has the same kinetics as a radical–radical dimerization.[9] It thus appears that, at these three pHs, reaction p can be considered as an equilibrium connecting the participation of the α-hydroxymethyl and ketyl radicals to the homo- and heterodimerizations d1, d2, and d3. This is not the case at pH 8.2 where the peak potential of the first wave varies by 30 mV per decade of scan rate, indicating that the rate control is by a first-order step following the electron-transfer step, i.e., forward reaction p in the framework of the mechanism depicted in Scheme I.

Upon raising the scan rate, reversibility or partial reversibility for the first peak can be reached below 1000 V s^{-1} at pH 12 and 11, whereas no trace of reversibility appears up to this value of the scan rate at pH 10.2 and 8.2. This is qualitatively consistent with the expectation that reaction d1 should be slower, because

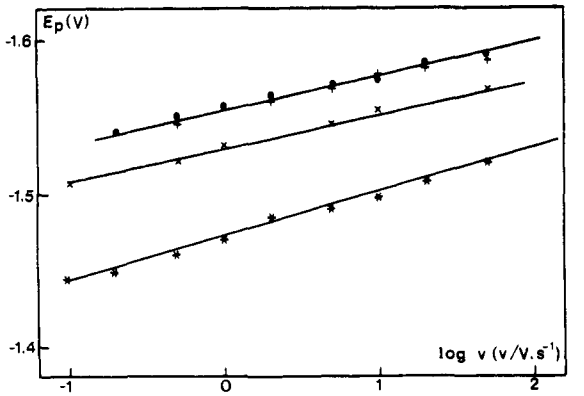

Figure 3. Cyclic voltammetry of benzaldehyde (2 mM) in ethanol at a hanging mercury drop electrode. Variations of the peak potential of the first wave with the scan rate at pH 8.2 (*), 10.2 (×), 11 (●), 12 (+). Temperature: 25 °C.

of Coulombic repulsion of the two negative charges, than reactions d2 and d3. From these data and their simulation, it was found that the standard potential $E_1^0 = -1.55_2$ V vs SCE and that the overall dimerization constant

$$k_D = \frac{2}{(1 + K_p)^2}(k_1 + k_2K_p + k_3K_p^2) \qquad (1)$$

is equal to 3.9×10^5 and 9.7×10^5 M^{-1} s^{-1} at pH 12 and 11, respectively. From the peak potential of the first irreversible wave (E_1^p) at pH 10.2 (Figure 2) and the following relationship (see the Appendix and ref 9)

$$E_1^p = -0.902\frac{RT}{F} + E_1^0 + \frac{RT}{F}\ln\left[(1 + K_p)\left(\frac{2}{3}\frac{RT}{F}C^0\frac{k_D}{v}\right)^{1/3}\right]$$

it was found that

$$(1 + K_p)^3 k_{D,pH\,10.2} = 3.6 \times 10^6 \text{ M}^{-1} \text{ s}^{-1}$$

and from the value of E_1^p at pH 8.2 (Figure 2) with[9]

$$E_1^p = -0.780\frac{RT}{F} + E_1^0 + \frac{RT}{2F}\ln\left(\frac{k_p}{v}\frac{RT}{F}\right)$$

that

$$k_{p,pH\,8.2} = 2.0 \times 10^6 \text{ M}^{-1} \text{ s}^{-1}$$

As seen before at pH 12, there is practically no conversion of the ketyl radical into the α-hydroxybenzyl radical, i.e., $K_p \ll 1$. It follows that

$$k_1 = \frac{1}{2}k_{D,pH\,12} = 2 \times 10^5 \text{ M}^{-1} \text{ s}^{-1}$$

As will be made clear in the following, $K_p \ll 1$ also at pH 11 and 10.2. Thus,

$$\frac{k_2}{K_A} + 10^{-11}\frac{k_3}{K_A^2} = 2.9 \times 10^{16} \text{ M}^{-2} \text{ s}^{-1}$$

$$\frac{k_2}{K_A} + 10^{-10.2}\frac{k_3}{K_A^2} = 2.5 \times 10^{16} \text{ M}^{-2} \text{ s}^{-1}$$

It appears from these two equations that the second term on the left-hand side is negligible and that

$$\frac{k_2}{K_A} = 2.7 \times 10^{16} \text{ M}^{-2} \text{ s}^{-1} \qquad (2)$$

The simulation of the whole cyclic voltammetric curves, including the first wave where the ketyl and hydroxybenzyl radicals are formed and the further waves where these radicals are reduced, according to the mechanism shown in Scheme I, would be rather cumbersome and would depend upon a large number of parameters

(9) Andrieux, C. P.; Savéant, J.-M. *Electrochemical Reactions in Investigation of Rates and Mechanisms of Reactions, Techniques of Chemistry*; Bernasconi, C. F., Ed.; Wiley: New York, 1986; Vol. VI/4E. Part 2, pp 305–390.

(10) Andrieux. C. P.; Grzeszczuk, M.; Savéant. J.-M. *Electroanal. Chem.*, in press.

in the general case. Fortunately, the following simplifying conditions are achieved. Since we aim at simulating the cyclic voltammograms under conditions of chemical irreversibility (Figure 1), the concentrations of the two transient radicals significantly differ from zero only within a thin reaction layer adjacent to the electrode surface, much thinner than the diffusion layer of the substrate. This is true for all four buffers. In addition, for the three most basic buffers, it has already been noted that at the first wave the kinetics are formally those of a radical–radical dimerization process. This means that the reaction layer should in fact be divided into two sublayers of quite different thicknesses, pertaining to the protonation reaction p on the one hand and to the three dimerization reactions (d1, d2, d3) on the other. In the first sublayer, adjacent to the electrode surface and much thinner than the second, reaction p may significantly depart from equilibrium, and the dimerization steps are not yet effective. In the remainder of the total reaction layer, the departure of reaction p from equilibrium has become negligible, and the various dimerization steps may effectively take place. Under these conditions, as shown in the Appendix, the current–potential curves are predicted to depend upon the following parameters. The equation

$$E_1^* = E_1^0 + \frac{RT}{F}\ln\left[(1+K_p)\left(\frac{2RT\,k_D C^0}{3Fv}\right)^{1/3}\right]$$

governs the location of the first wave (k_D is the same as defined in eq 1), while

$$E_2^* = E_2^0 + \phi_r\left(1+\frac{1}{\alpha_2}\right) + \frac{RT}{\alpha_2 F}\ln\left[\frac{k_2^S}{(FvD/RT)^{1/2}}\,\frac{1}{1+K_p}\,\frac{1}{(2\,RT\,k_D C^0/3Fv)^{1/3}}\right]$$

governs the location of the wave representing the reduction of the ketyl radical[10] and

$$E_3^* = E_3^0 + \phi_r + \frac{RT}{\alpha_3 F}\ln\left[\frac{k_3^S}{(FvD/RT)^{1/2}}\,\frac{K_p}{1+K_p}\,\frac{1}{(2\,RTk_D C^0/3Fv)^{1/3}}\right]$$

that of the α-hydroxybenzyl radical.[10] The relative height of the reduction wave of the α-hydroxybenzyl and ketyl radicals is controlled by the parameter

$$\gamma = \left(\frac{2}{3}\right)^{1/3}\left(\frac{Fv}{RT}\right)^{1/6} C^{0\,1/3}\frac{k_D^{1/3}}{K_p(k_p[DH] + k_{-p}[D^-])^{1/2}}$$

(C^0 is the concentration of substrate and v the scan rate.) At high pHs, for example at pH 12, γ is large and the second wave represents the reduction of the ketyl radical. γ decreases with the pH, and thus at pH 10.2 the second wave represents the reduction of α-hydroxybenzyl radical with negligible interference by the reduction of the ketyl radical. An intermediary situation is observed at pH 11 where the second wave is split into two subwaves representing the reduction of the α-hydroxybenzyl radical first and then that of the ketyl radical. The relative amount of α-hydroxybenzyl radical need not be large for a significant reduction wave to be observed, since it is reduced at a less negative potential than the ketyl radical and since the protonation reaction is likely to be fast. Kinetically controlled regeneration of the α-hydroxybenzyl radical from protonation of the ketyl radical then enhances the reduction wave of the former over the height that would correspond to their equilibrium ratio.

The results of the simulation of the voltammograms are shown in Figure 1 for the three most basic buffers; we have used the procedure outlined above and in the Appendix. Satisfactory simulation of the experimental curves was reached for the following values of the parameters.

At pH 12, $E_2^* = -2.01_3$ V vs SCE and $\alpha_2 = 0.4$. It follows that the "reduction potential" of the ketyl radical, defined as

$$E_2^S = E_2^0 + \phi_r\left(1+\frac{1}{\alpha_2}\right) + \frac{RT}{\alpha_2 F}\ln\left[\frac{k_2^S}{\left(\frac{FvD}{RT}\right)^{1/2}}\right]$$

is equal (at 1 V s^{-1}) to -1.95_7 V vs SCE. Thus, assuming the validity of the Marcus–Hush quadratic law and applying the ensuing equations,[11] it is found that[12] (taking $Z^{el} = 4\times10^3$ cm s^{-1}, $D = 10^{-5}$ cm^2 s^{-1}) $E_2^0 - 0.25\phi_r = -1.64_8$ V vs SCE, and $\Delta G^{\ddagger}_{0.2} = 0.45_6 + 1.56\phi_r$ (eV).

(11) (a) These two characteristic potentials were derived under the assumption that the electron transfer to both the ketyl and the α-hydroxybenzyl radicals obey the Butler–Volmer law. As shown before, this is a perfectly reasonable approximation along the wave obtained at a single scan rate,[3] even though the electron transfer is likely to be best represented by a quadratic law of the Marcus–Hush type,[11b,c] i.e.,

$$\Delta G^{\ddagger} = z\phi_r + \Delta G_0^{\ddagger}\left(1+\frac{E - E^0 - \phi_r}{4\Delta G_0^{\ddagger}}\right)^2$$

$\Delta G^{\ddagger}$ and $\Delta G_0^{\ddagger}$ are the activation and standard activation free energies, respectively, expressed in electronvolts, E and E^0 the electrode potential and standard potential expressed in volts, and ϕ_r is the potential difference between the reaction site and the solution, also in volts, z is the charge number of the reactant. Since the transfer coefficient (symmetry factor)

$$\alpha = \frac{\partial\Delta G^{\ddagger}}{\partial E} = \frac{1}{2}\left(1+\frac{E - E^0 - \phi_r}{4\Delta G_0^{\ddagger}}\right)$$

does not vary significantly along the reduction wave, $\Delta G^{\ddagger}$ can be linearized, thus leading to

$$\Delta G^{\ddagger} = 4\alpha(1-\alpha)\,\Delta G_0^{\ddagger} + \alpha\left[E - E^0 - \phi_r\left(1-\frac{z}{\alpha}\right)\right]$$

Thus, in the Butler–Volmer law:

$$\frac{i}{FS} = k^S\exp\left\{-\frac{\alpha F}{RT}\left[E - E^0 - \phi_r\left(1-\frac{z}{\alpha}\right)\right]\right\}C_0$$

(i, current; S, electrode surface area; C_0, concentration of the reactant at the electrode surface).

$$\Delta G_0^{\ddagger} = \frac{RT}{4\alpha(1-\alpha)F}\ln\left(\frac{Z^{el}}{k^S}\right)$$

where Z^{el} is the electrochemical collision frequency.

Defining E^R as

$$E^R = E^0 + \phi_r\left(1-\frac{z}{\alpha}\right) + \frac{RT}{\alpha F}\ln\left[\frac{k^S}{\left(\frac{FvD}{RT}\right)^{1/2}}\right]$$

it follows that

$$E^0 + \left(1 + z\frac{1-2\alpha}{\alpha^2}\right)\phi_r = E^R + \frac{1-\alpha}{\alpha}(E - E^R) + \frac{1-2\alpha}{\alpha^2}\frac{RT}{F}\ln\left[\frac{Z^{el}}{\left(\frac{FvD}{RT}\right)^{1/2}}\right]$$

and

$$\Delta G_0^{\ddagger} = -\frac{z\phi_r}{4\alpha^2} + \frac{(E - E^R)}{4\alpha} + \frac{RT}{4\alpha^2 F}\ln\left[\frac{Z^{el}}{\left(\frac{FvD}{RT}\right)^{1/2}}\right]$$

In the present case E is to be taken as equal to E^* for each of the second waves. (b) Marcus, R. A. *J. Chem. Phys.* **1956**, *24*, 4966. (c) Hush, N. S. *J. Chem. Phys.* **1958**, *28*, 962.

(12) (a) The formation of the dianion from the reduction of the ketyl radical is accompanied by a protonation reaction that certainly possesses a large driving force. It may sequentially follow the electron-transfer step, but it is also conceivable that a molecule of water or ethanol may be H-bonded to the ketyl radical and that proton transfer be concerted with electron transfer. (b) As compared to the standard potential, the potential where the second wave takes place is the result of three different shifts: two negative shifts caused by the slowness of the electron transfer and by the competition with the dimerization process and a positive shift caused by the rapid protonation of the anion formed upon electron transfer to the α-hydroxybenzyl radical. These shifts compensate each other accidentally in the present case.

Scheme I

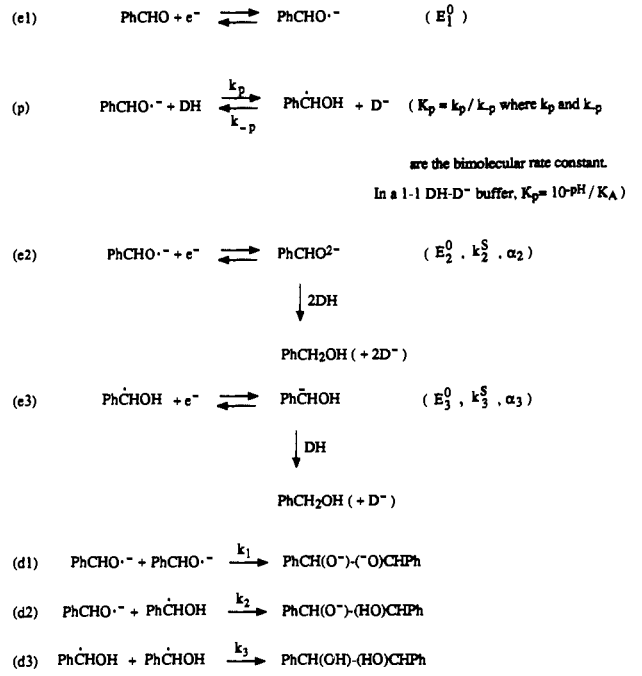

At pH 11, the relative magnitude of the two second waves at 1 V s^{-1} is such that $\gamma = 1$. It follows from the value of k_D derived from the first waves ($k_{-p}[D^-] \gg k_p[DH]$, $[D^-] = 0.1$ M) that

$$\frac{(k_{-p})^{1/2}}{K_A} = 6.3 \times 10^{12}\ M^{-3/2}\ s^{-1/2} \qquad (3)$$

At pH 10.2, $E_3^* = -1.79_4$ V vs SCE and $\alpha_3 = 0.42$. It follows, from the relationship that defines E_3^*, that the "reduction potential" of the α-hydroxybenzyl radical (resulting from the thermodynamics and kinetics of the electron transfer step to the exclusion of the kinetics of accompanying chemical steps),

$$E_3^R = E_3^0 + \phi_r + \frac{RT}{\alpha_3 F} \ln \left[\frac{k_3^S}{\left(\frac{FvD}{RT}\right)^{1/2}} \right]$$

at 1 V s^{-1} is such that

$$E_3^R + \frac{RT}{\alpha_3 F} \ln \frac{10^{-10.2}}{K_A} = -1.69_6 \text{ V vs SCE} \qquad (4)$$

At pH 8.2, the simplifications we have used to simulate the current–potential curves in the three other buffers are no longer strictly valid, since the first wave is kinetically controlled by the protonation of the ketyl radical. At the second wave, the kinetic situation corresponds to conditions that are in between those that were valid in the three other buffers (the protonation equilibrium is assumed to be achieved as far as the dimerizations are concerned), and conditions in which the ketyl radical would be immediately converted into the α-hydroxybenzyl radical ($K_p \gg 1$) and its reduction would compete with its self-dimerization (reaction e3). In both cases the formal kinetics are the same, what differs is simply the value of k_D: k_D has the expression given in eq 1 in the first case, and $k_D = 2k_3$ in the second. The voltammogram (Figure 1) was thus simulated with a first wave controlled by reaction p and giving rise to a dimerizing intermediate. A good fit (Figure 1) with the experimental data was found for $E_3^* = -1.65_7$ V vs SCE and $\alpha_3 = 0.5$.

Assuming again the validity of the Marcus–Hush quadratic law, the fact that $\alpha_3 = 0.5$ indicates that[11b]

$$E_3^0 + \phi_r = E_3^* = -1.65_7 \text{ V}$$

Since ϕ_r is not likely to vary significantly from pH 8.2 to 10.2, the same value of $E_3^0 + \phi_r$ can be used at pH 10.2. At this latter pH, $E_3^* = -1.79_4$ V vs SCE, and thus the driving force of the electron transfer to the α-hydroxybenzyl radical is -0.13_7 eV. The standard activation free energy, $\Delta G_{0,3}^{\ddagger}$, can thus be derived from the value of α_3 (0.42) by using

$$\alpha_3 = 0.5 \left(1 - \frac{0.137}{4\Delta G_{0,3}^{\ddagger}} \right)$$

We then find that $\Delta G_{0,3}^{\ddagger} = 0.21_4$ eV. It follows that[11] $k_3^S = 1.2$ cm s^{-1} and thus that $E_3^R = -1.40_6$ V vs SCE. We thus obtained from eq 4 the value of the pK_A of the α-hydroxybenzyl radical: $pK_A = 8.1_4$. The value of k_2 is then obtained from eq 2: $k_2 = 2.0 \times 10^8\ M^{-1}\ s^{-1}$.

If we now come back to the results at pH 8.2, from the values of $\Delta G_{0,3}^{\ddagger}$ and $E_3^0 + \phi_r$ just determined and taking into account that $\alpha_3 = 0.5$, we obtain $E_{3,pH\,8.2}^R = -1.45_7$ V vs SCE. From $E_3^* = -1.65_7$ and $\alpha_3 = 0.5$, we can now estimate k_3. With the first of the two approximations made previously, we obtain $k_3 = 0.6 \times 10^9\ M^{-1}\ s^{-1}$, whereas with the second of two, $k_3 = 1.7 \times 10^9\ M^{-1}\ s^{-1}$, i.e., two values that are of the same order of magnitude.

Since we now know the value of the pK_A of the α-hydroxybenzyl/ketyl radical couple, it is possible to derive the values of the protonation and deprotonation rate constants at pH 11 from eq 3: $k_{p,pH\,11} = 2.9 \times 10^6\ M^{-1}\ s^{-1}$ and $k_{-p,pH\,11} = 2.1 \times 10^9\ M^{-1}\ s^{-1}$.

The values of the various thermodynamic and kinetic constants thus derived are summarized in Table I.

In the potential region of interest, the potential at the reaction site, ϕ_r, is of the order −0.1 V. Thus the standard potential for the reduction of the ketyl radical into the dianion would be only ca. 120 mV more negative than that of the α-hydroxybenzyl radical. This lends support to the possibility that electron transfer to the ketyl radical be concerted with proton transfer as already envisaged.[12a] If this is correct, the standard potential for the direct reduction of the ketyl radical into the monoanion would be ca. 120 mV more negative than for the reduction of the α-hydroxybenzyl radical, and it would be intrinsically slower by about 0.1 eV in terms of standard activation free energy as expected from the contribution of proton transfer to the intrinsic barrier.

The determination of the pK_A of the α-hydroxybenzyl/ketyl radical acid–base couple hinges indirectly upon the assumption that electron transfer to the α-hydroxybenzyl radical follows a Marcus–Hush type kinetics. An alternative approximate approach would be to assume that the reduction potential of the α-hydroxybenzyl radical does not vary between pH 10.2 and 8.2 and that the rate constants of the dimerization steps d2 and d3 are the same. This would lead to a pK_A value of 8.7, which is not dramatically different from what was found by using the above more rigorous approach.

As expected from the Coulombic repulsion between the two ketyl radicals, their self-dimerization is quite significantly slower than their cross-dimerization with the α-hydroxybenzyl radicals or than the self-dimerization of the latter. The self-dimerization

Table I. Thermodynamic and Kinetic Constants[a]

Electron Transfer Reactions
$E^0_{PhCHO/PhCHO^{\cdot-}} = -1.55_2$
$E^0_{PhCHO^{\cdot-}/PhCHO^{2-}} - 0.25\phi_r = -1.64_8$
$E^0_{PhĊHOH/PhĊHOH} + \phi_r = -1.657$
$\Delta G^{\ddagger}_{0,PhCHO^{\cdot-}/PhCHO^{2-}} = 0.45_6 + 1.56\phi_r$
$\Delta G^{\ddagger}_{0,PhĊHOH/PhĊHOH} = 0.21_4$
Proton Transfer Reaction
$pK_{A,PhĊHOH/PhCHO^{\cdot-}} = 8.1_4$
$k_{p,pH\,8.2} = 4.2 \times 10^9$, $k_{-p,pH\,8.2} = 5.8 \times 10^6$
$k_{p,pH\,11} = 2.9 \times 10^6$, $k_{-p,pH\,11} = 2.1 \times 10^9$
Dimerization Reactions
$k_1 = 2.0 \times 10^5$
$k_2 = 2.0 \times 10^8$
$k_3 \approx 10^9$

[a] Standard potentials E^0 in volts vs SCE, standard activation free energies $\Delta G_0^{\ddagger}$ in electronvolts, rate constants in $M^{-1}\ s^{-1}$.

of α-hydroxybenzyl radicals is somewhat faster than their cross-dimerization with the ketyl radicals. This falls in line with the fact that the driving force is larger in the first case than in the second by the same amount as the difference in pK_A between one alcoholic function in the pinacol and the α-hydroxybenzyl radical (i.e., by at least 4 units).

The above quantitative analysis confirms the assignment of the second wave observed at pH 8.2 and 10.2 and of the first of the two second waves at pH 11 to the reduction of the α-hydroxybenzyl radical. The latter clearly appear to be more difficult to reduce than the starting benzaldehyde. The same reasons that cause this ordering of the reduction potentials of the α-hydroxybenzyl radical and benzaldehyde are also responsible for the noninterference of the homogeneous electron transfer between the ketyl radical and the α-hydroxybenzyl radical

$$PhCHO^{\bullet-} + PhCHOH \rightleftarrows PhCHO + Ph\dot{C}HOH \quad (e4)$$

that would have caused, through regeneration of benzaldehyde, the first wave to be a two-electron wave unlike what is observed experimentally. If it were to interfere, reaction e4 would be followed by the fast protonation of the anion thus formed. The maximal efficiency of this disproportionation process would be reached under conditions where this protonation step would be faster than backward reaction e4, i.e., when forward reaction e4 would be the rate-determining step. Its maximal rate constant may be estimated as follows from the heterogeneous rate data gathered previously. As with many other organic molecules, the reduction of the α-hydroxybenzyl radicals is likely to behave in between the predictions of the Marcus model and the Hush model.[4b,13] In the first of these models, the image force effect is taken into account and the reactant considered to be at a distance from the electrode equal to its radius. Under these conditions, the homogeneous self-exchange activation free energy is twice the electrochemical standard activation free energy, i.e., 0.42_8 eV. On the other hand, the self-exchange activation free energy of the PhCHO/PhCHO$^{\bullet-}$ couple is, under the same approximation, 0.46_3 eV.[13] It follows that the intrinsic barrier for reaction e4 is 0.44_6 eV. Since the difference in standard potentials of the two couples is close to zero, the rate constant of reaction e4 can be estimated to be ca. 10^4 M^{-1} s^{-1} (taking 3×10^{11} M^{-1} s^{-1} for the homogeneous collision frequency), i.e., much lower than those of the dimerizations in which the α-hydroxybenzyl radical is involved. In the Hush model, the reacting site is considered to be located far from the electrode surface and the image forces are neglected. Under these conditions, the homogeneous self-exchange activation free energy is the same as the electrochemical standard activation free energy, i.e., 0.21_4 eV. The intrinsic barrier for reaction e4 would then be 0.20_7 eV. Since the reacting site is far from the electrode, this amounts to neglecting ϕ_r in the estimation of the standard potential. Reaction e4 would then be an uphill process (by 10_5 meV). It follows that the rate constant of reaction e4 would be of the order 5×10^6 M^{-1} s^{-1}, again clearly smaller than the rate constants of the α-hydroxybenzyl radical dimerizations.

The mechanism previously[7d] proposed for the electrodimerization reaction taking place at the first wave of benzaldehyde in media such as those investigated here is thus essentially correct, in the sense that it explained the acceleration of the followup reaction observed upon decreasing the pH by the participation of the α-hydroxybenzyl radical in the dimerization process. This mechanism has been criticized later on on the basis that the homogeneous electron transfer (e4), then believed to be very fast (close to the diffusion limit), should overrun the radical–radical coupling reactions (d1, d2, d3) as soon as the α-hydroxybenzyl radical is formed.[7h] Since, under these conditions, the apparent number of electrons remains equal to one, an alternative mechanism of the dimerization process was proposed involving the radical attack on the carbonyl double bond of benzaldehyde by the α-hydroxybenzyl radical

$$PhCHOH + PhCHO \rightarrow PhCH(\dot{O})(HO)CHPh \quad (d4)$$

followed by rapid reduction of the oxygen-centered radical.[7h,14] We now know that reaction e4 is not an actual competing pathway to the dimerization reactions involving the α-hydroxybenzyl radical. However, it remains for us to examine whether or not reaction d4 could successfully compete with reactions d2 and d3. This is quite unlikely since reaction d4 is in fact an uphill reaction as seen from the following analysis. From thermochemical literature data[15a] we can estimate the enthalpy of reaction d4 in the gas phase

$$\Delta H_{d4} = H_{PhCH(\dot{O})(HO)CHPh} - H_{PhCHO} - H_{Ph\dot{C}HOH}$$

(where the H's are the enthalpies of formation of the various species from the elements). $H_{PhCHO} = -6$ kcal/mol. $H_{Ph\dot{C}HOH}$ is obtained as follows:

$$H_{Ph\dot{C}HOH} = H_{CH_3\dot{C}HOH} + H_{PhCH_2\cdot} - H_{CH_3CH_2\cdot} = 1 \text{ kcal/mol}$$

Similarly, the formation enthalpy of PhCH(Ȯ)(HO)CHPh is estimated from that of $(CH_3)_2\dot{C}HO^{\bullet}$ by the incremental method leading to PhCH(Ȯ)(HO)CHPh = 6.7 kcal/mol. It is thus found that the reaction is endothermic by 14 kcal/mol (0.6 eV). There is not enough data available to estimate the reaction entropy precisely. However, since a dimer is formed there is a loss of entropy that can be estimated as being on the order of 10 eu.[15b] The standard free energy of the reaction is thus on the order 17 kcal/mol (0.75 eV).

Another procedure for estimating the standard free energy of the reaction is the following (the μ^0's are the standard free enthalpy of formation from the elements):

$$\Delta G^0_{d4} = [\mu^0_{PhCHC(\dot{O})(HO)CHPh} - \mu^0_{H\cdot} - \mu^0_{PhCH(OH)(HO)CHPh}] + [\mu^0_{PhCH(OH)(HO)CHPh} - 2\mu^0_{Ph\dot{C}HOH}] + \frac{1}{2}\mu^0_{H_2} - \mu^0_{H\cdot} + E^0_{H^+ + e^-/1/2H_2} - E^0_{PhCHO + e^- + H^+/Ph\dot{C}HOH}$$

Neglecting the enthropy terms in the two first brackets, we find 104 and 48 kcal/mol respectively, 52 kcal/mol for the third terms, whereas the difference of the last two terms can be estimated as equal to −0.82 V. Overall, $\Delta G^0 = 23$ kcal/mol (1 eV). Both estimations lead to similar results, showing that the reaction is significantly endergonic and is thus quite unlikely to compete, on kinetic grounds, with the dimerization steps d2 and d3, which are largely exergonic reactions.

Conclusion

The present study has unambiguously shown that the α-hydroxybenzyl radical obtained from the one-electron + one-proton electrochemical reduction of benzaldehyde is more difficult to reduce than the starting molecule. It offers a clear example of the lack of general validity of the commonly accepted rule, according to which neutral radicals resulting from proton addition on initially formed anion radicals should be easier to reduce than the substrate. Further evidence is thus provided that electrochemical means may well be effective for triggering radical reactions as well as for investigating the redox properties of the radicals thus generated.

Experimental Section

Chemicals. Ethanol, n-Bu_4NClO_4, n-Bu_4NOH (40% aqueous solution), 2,6-dimethylphenol, and veronal were from commercial origin and used as received. Phenol and benzaldehyde, from commercial origin, were distilled under reduced pressure before use.

Instrumentation. The cyclic voltammetric experiments were carried out in a thermostated (25 °C) three-electrode cell. The working electrode was a mercury drop hanged on a 1-mm diameter gold disk. The refer-

(13) Investigation of the first wave at pH 12 using large scan rates revealed that the electrochemical ΔG^*_5 is equal to 0.23 eV.[10]

(14) (a) The discussion was based on the kinetic analysis of the first wave in ethanolic acetate buffers. No direct proof of the occurrence of reaction d4 could be obtained since the protonation of the ketyl radical is then the rate-determining step. The latter observation falls in line with what we have found in our most acidic buffer (veronal). (b) In order to overrun reaction e4 assumed to be at the diffusion limit (10^9–10^{10} M^{-1} s^{-1}), reaction d4 would also have to be a very fast reaction.

(15) (a) Benson, S. W. *Thermodynamical Kinetics*, 2nd ed.; Wiley: New York, 1976. (b) Savéant, J.-M. *Acta Chem. Scand. B* **1988**, *42*, 721.

ence electrode was an aqueous saturated calomel electrode separated from the solution by a bridge filled with the ethanolic solution under investigation. The counterelectrode was a platinum wire.

The cyclic voltammetry apparatus was composed of a home-built solid-state amplifier potentiostat with positive feedback iR drop compensation[16] and a PAR (Model 175) function generator. The voltammograms were displayed on a chart recorder (Ifelec 2502) for sweep rates below 0.5 V s^{-1} and, for higher sweep rates, on a Nicolet (3091) digital oscilloscope.

Appendix

The kinetics of the set of reactions in Scheme I are governed by the following set of partial derivative equations and boundary and initial conditions.

$$\frac{\partial a}{\partial \tau} = \frac{\partial^2 a}{\partial y^2}$$

$$\frac{\partial b}{\partial \tau} = \frac{\partial^2 b}{\partial y^2} - \lambda_p b + \lambda_{-p} c - 2\lambda_1 b^2 - \lambda_2 bc$$

$$\frac{\partial c}{\partial \tau} = \frac{\partial^2 c}{\partial y^2} + \lambda_p b - \lambda_{-p} c - \lambda_2 bc - 2\lambda_3 c^2$$

When $\tau = 0, y \geq 0$ and $y = \infty, \tau \geq 0$: $a = 1, b = 0, c = 0$. When $y = 0, \tau \geq 0$:

$$a = b \exp\left[\frac{F}{RT}(E - E_1^0)\right]$$

$$\psi_2 = \exp\left[\frac{-\alpha_2 F}{RT}(E - E_2^R)\right] b, \quad \psi_3 = \exp\left[\frac{-\alpha_3 F}{RT}(E - E_3^R)\right] c$$

$$\left[\frac{\partial a}{\partial y}\right]_{y=0} = \psi_1, \quad \left[\frac{\partial b}{\partial y}\right]_{y=0} = \psi_2 - \psi_1, \quad \left[\frac{\partial c}{\partial y}\right]_{y=0} = \psi_3$$

$$\psi = \psi_1 + \psi_2 + \psi_3$$

$$E_2^R = E_2^0 + \frac{RT}{\alpha_2 F}, \quad E_3^R = E_3^0 + \frac{RT}{\alpha_3 F}$$

The various dimensionless variables in the above equations have the following definitions: t, is the time, x, the distance from the electrode surface (the diffusion to and from the electrode is assumed to be linear and semiinfinite), D, the diffusion coefficient (assumed to be the same for all species), C^0, the concentration of the substrate in the bulk of the solution, E_1^0, E_2^0, E_3^0 the standard potentials, E, the electrode potential, v, the scan rate ($E = E_i - vt$, the initial potential E_i being large enough compared to E_1^0 for the difference between them to be regarded as mathematically infinite), k_p, k_{-p}, k_1, k_2, and k_3 the rate constants of the corresponding reactions.

$$\tau = \frac{Fv}{RT}t, \quad \xi = -\frac{F}{RT}(E - E_1^0), \quad y = x\left(\frac{Fv}{RTD}\right)^{1/2}$$

a, b, and c are the concentrations of PhCHO, PhCHO$^{\bullet-}$, and PhĊHOH normalized toward C^0,

$$\psi = \frac{i}{FSC^0 D^{1/2}(Fv/RT)^{1/2}}$$

is the dimensionless expression of the total current (i, current; S, electrode surface area) ψ_1, ψ_2, and ψ_3 are the contributions of the reduction of PhCHO, PhCHO$^{\bullet-}$, and PhĊHOH to the current, respectively. The various kinetic constants are defined as

$$\lambda_p = \frac{RT}{F}\frac{k_p[DH]}{v}, \quad \lambda_{-p} = \frac{RT}{F}\frac{k_{-p}[D^-]}{v}, \quad \frac{\lambda_p}{\lambda_{-p}} = K_p$$

$$\lambda_1 = \frac{RT}{F}\frac{k_1 C^0}{v}, \quad \lambda_2 = \frac{RT}{F}\frac{k_2 C^0}{v}, \quad \lambda_3 = \frac{RT}{F}\frac{k_3 C^0}{v}$$

Under the simplifying conditions defined in the text, the above system of equations can be replaced by

$$0 = \frac{\partial^2 (c - K_p b)}{\partial y^2} - (\lambda_p + \lambda_{-p})(c - K_p b)$$

in the first reaction sublayer

$$0 = \frac{\partial^2 b + c}{\partial y^2} - \lambda_D (b + c)^2$$

with $c = K_p b$ in the remainder of the reaction layer and $\lambda_D = RT k_D C^0/Fv$. Integration of these two equations and that pertaining to a, taking account of the initial and boundary conditions, leads to the following integral equation expressions of the three contributions to the dimensionless current.

$$(1 - I\psi_1)\exp(\xi) = \left\{\psi_1 - (1 - I\psi_1)\exp(\xi)\left[\exp[\alpha_2(\xi + \Delta\xi_2)] + \frac{1}{\gamma + \exp[\alpha_3(\xi + \Delta\xi_3)]}\right]\right\}^{2/3}$$

$$\psi_2 = (1 - I\psi_1)\exp(\xi)\exp[\alpha_2(\xi + \Delta\xi_2)],$$

$$\psi_3 = \psi_2 \frac{\exp[-\alpha_2(\xi + \Delta\xi_2)]}{\gamma + \exp[-\alpha_3(\xi + \Delta\xi_3)]}$$

where

$$\xi = -\frac{E}{RT}(E - E_1^*), \quad \Delta\xi_2 = -\frac{F}{RT}(E_1^* - E_2^*),$$

$$\Delta\xi_3 = -\frac{F}{RT}(E_1^* - E_3^*)$$

E_1^*, E_2^*, E_3^*, and γ being the same as defined in the text and where

$$I\psi_1 = \int_{-\infty}^{\xi} \frac{\psi_1}{(\xi - \eta)^{1/2}} d\eta$$

The simulations of the cyclic voltammograms in Figure 1 were carried out by numerical resolution of the above equations according to usual procedures.[3]

Registry No. PhCHO, 100-52-7; PhCHO$^{\bullet-}$, 34473-57-9; PhC$^{\bullet}$HOH, 2406-15-7.

(16) Garreau, D.; Savéant, J.-M. *J. Electroanal. Chem.* **1977**, *99*, 2786.